Published in final edited form as:
Biochem Biophys Res Commun. 2012 June 22; 423(1): 13–18. doi:10.1016/j.bbrc.2012.05.042.

Blockade of β-cell K_{ATP} channels by the endocannabinoid, 2-arachidonoylglycerol

Charles E. Spivak[1], **Wook Kim**[2], **Qing-Rong Liu**[3], **Carl R. Lupica**[1], and **Máire E Doyle**[4]

[1]Cellular Neurobiology Branch, Electrophysiology Research Section, National Institute on Drug Abuse, National Institutes of Health, Baltimore, MD 21224, USA

[2]Laboratory of Clinical Investigation, National Institute on Aging, National Institutes of Health, Baltimore, MD 21224, USA

[3]Behavior Neuroscience Branch, National Institute on Drug Abuse, National Institutes of Health, Baltimore, MD 21224, USA

[4]Johns Hopkins Medical Institutes, Johns Hopkins Bayview, Department of Medicine, Division of Endocrinology, Baltimore, MD 21224, USA

Abstract

The endocannabinoid system has been demonstrated to be active in the pancreatic β-cell. However the effects of the endocannabinoids (ECs) on insulin secretion are not well defined and may vary depending on the metabolic state of the β-cell. Specifically it is not known whether the effects of the ECs occur by activation of the cannabinoid receptors or via their direct interaction with the ion channels of the β-cell. To begin to delineate the effects of ECs on β-cell function, we examined how the EC, 2-AG influences β-cell ion channels in the absence of glucose stimulation. The mouse insulinoma cell line R7T1 was used to survey the effects of 2-AG on the high voltage activated (HVA) calcium, the delayed rectifier (K_v), and the ATP-sensitive K (K_{ATP}) channels by whole cell patch clamp recording. At 2 mM glucose, 2-AG inhibited the HVA calcium (the majority of which are L-type channels), K_v, and K_{ATP} channels. The channel exhibiting the most sensitivity to 2-AG blockade was the K_{ATP} channel, where the IC_{50} for 2-AG was 1μM. Pharmacological agents revealed that the blockade of all these channels was independent of cannabinoid receptors. Our results provide a mechanism for the previous observations that CB1R agonists increase insulin secretion at low glucose concentrations through CB1R independent blockade of the K_{ATP} channel.

Keywords

β-cell; endocannabinoid; receptor independent effects; insulinoma cell line; low glucose

Corresponding Author: Máire E. Doyle, PhD, Division of Endocrinology, JHBMC, 5200 Eastern Avenue, MFL Building, Center Tower, 4th Fl., Rm 4300, Baltimore, MD 21224, Phone: 1-410-550-8484, Fax: 1-410-550-6864, mdoyle1@jhmi.edu.

1. Introduction

Endogenous cannabinoids (endocannabinoids, ECs) are lipid signaling molecules derived from arachidonic acid.[1] They are synthesized *in situ* only on demand by catabolism of phospholipids of the cell membrane and are rapidly degraded.[1] Actions of the two major ECs, 2-arachidonoylglycerol (2-AG) and anandamide (AEA), are primarily mediated by two specific G protein-coupled receptors, the cannabinoid 1 and cannabinoid 2 receptors (CB1R and CB2R respectively).[2,3] The activity of the enzymes catalyzing the final steps of EC synthesis, diacylglycerol lipase (DAGL) alpha and beta and N-acyl-phosphatidyl ethanolamine-hydrolyzing phospholipase (NAPE-PLD) for 2-AG and AEA, respectively, are calcium sensitive [2] We and others have shown that the ECs and the enzymes for their synthesis and degradation are present in the β-cell.[4,5] Insulin secretion is initiated by closure of the K_{ATP} channel, subsequent cell membrane depolarization, opening of the L-type calcium channel and influx of calcium to stimulate exocytosis of the insulin granules. Given the dependence of the enzymes for EC synthesis on calcium we postulated that EC synthesis would be stimulated by β-cell membrane depolarization. We and others have shown that ECs are released directly in response to glucose-induced β-cell depolarization. [4,5] This obligate synthesis and release of ECs upon insulin exocytosis would imply that ECs could have a regulatory role in the initial steps of insulin secretion.

As β-cells are electrically excitable we hypothesized that some of the effects of the ECs on insulin secretion could be mediated via modulation of the ion channels regulating β-cell depolarization. Several precedents for direct action of the ECs on voltage-dependent and ligand gated ion channels have been set in other cell types.[6] Recent experimental evidence indicates that the metabolic state of the β-cell is important, as different effects were achieved at low and high glucose levels with CB1R agonists.[4,7,8] Therefore we reduced our examination of the effects of ECs on insulin secretion to the study of how the ECs modulate β-cell ion channels in the absence of stimulation. Thus, we examined the effects of the EC 2-AG, (the EC released in greater amounts from the islet)[4] on the ion channels involved in initiating insulin secretion using the highly differentiated R7T1 cell line under low glucose conditions.

2. Materials and Methods

2.1 R7T1 mouse insulinoma cell line

The cells, a gift from Dr. Nicholas Simpson (College of Medicine, University of Florida), were maintained in DMEM supplemented with 10% fetal calf serum, 2 mM L glutamine, 100 units of penicillin/mL, and 100 μg streptomycin/mL. In this cell line doxycycline (1 μg/mL) arrests differentiation and was used to propagate the line. All experiments were performed on cells cultured in the absence of doxycycline for at least one day. The cells were maintained in a humidified air/CO_2, 95/5 % incubator at 37°C.

2.2 Delayed rectifier currents

Whole cell voltage clamp of the R7T1 cell line used a bath solution of the following composition (mM): NaCl 150, KCl 5, $CaCl_2$ 2, $MgCl_2$ 1, NaH_2PO_4 1, HEPES 20, sorbitol 8, glucose 2; pH 7.40. The pipette solution consisted of (mM): KCl 120, $CaCl_2$ 1, $MgCl_2$ 1, HEPES 10, EGTA 10, MgATP 3, NaGTP 0.3; pH 7.20. Cells were held at a holding potential of −70 mV, then stepped to +50 mV using an Alembec VE-2 amplifier employing 100% series resistance compensation. The signals acquired after P/8 leak subtraction at about 1.5 min intervals, were low pass filtered at 5 kHz and sampled at 25 kHz. The measure of channel activity was the integral of the current signal.

2.3 High voltage activated (HVA) calcium currents

The bath solution consisted of (mM): NaCl 130, $BaCl_2$ 10, tetraethylammonium chloride (TEA) 20, $MgCl_2$ 1, HEPES 20, glucose 2; pH 7.40. The pipette solution consisted of (mM): cesium gluconate (120), TEA 20, $MgCl_2$ 2, HEPES 10, EGTA 10, MgATP 3, NaGTP 0.3; pH 7.20. Membrane potential was held at −60 mV then jumped to −10 mV to elicit the maximum calcium current using P/8 leak subtraction. The signal was filtered (low pass) at 5 kHz and sampled at 25 kHz. The integral of the current was taken as the response.

2.4 K_{ATP} single channel currents

K_{ATP} single channels were recorded in the R7T1 cell line using inside-out patches in a bath solution of the following composition (mM): KCl 110, $MgCl_2$ 1.44, EGTA 10, HEPES 10; pH 7.2 (KOH). The pipette solution (extracellular face) contained (mM) KCl 140, $CaCl_2$ 2.6, $MgCl_2$ 1.2, HEPES 10; pH 7.40. The pipette potential was maintained at +60 mV while a List Electronic EPC 7 amplifier recorded the data, which were filtered (low pass Bessel) at 5 kHz and sampled at 25 kHz. Cumulative charge curves over time were derived from the single channel activity.

When only a single conductance level appeared, open channel probability, P_O, was calculated as the total channel open time as a fraction as the total duration of the record segment analyzed. Such patches were rare. When more than one conductance level appeared, open probability was evaluated using binomial analysis. For this analysis, the all-points histogram was fitted to a multiple Gaussian function consisting of equally spaced means, corresponding to single channel currents. The areas under all components, normalized to unity, were then fitted in MLAB (Civilized Software, Bethesda, MD) to the binomial equation by a least squares procedure to derive P_o.

The number of active channels (r) was taken from the maximum currents observed. Higher values of r were evaluated using the maximum log likelihood criterion [9], but this criterion rarely favored r values greater than the maximum current actually seen. When the predicted fit of the binomial distribution was suspect, we analyzed the data for multiple open probabilities using the generalized binomial distribution of Poisson [9] and comparing the fit using the log likelihood criterion.

2.5 RT-qPCR analysis

Total RNAs were extracted from mouse R7T1 insulinoma cell line and mouse pancreatic islet cells using the Trizol protocol. Single strand cDNA was synthesized from total RNA templates using SuperScriptTM III One-Step RT-PCR System (Invitrogen, Carlsbad, CA). For quantitative real time PCR assays, the exon-junction-specific primers and fluorescent Fam-labeled and minor grove binder conjugated probes (Forward: GTGCCGAGGGAGCTTCTG; Reverse primer: GGCTCAACGTGACTGAGAAAGA; TaqMan MGB probe: TGCGAAGGGGTTCC) of mouse CB1R gene was designed using Primer Express (Applied Biosystems, Foster City, CA). Pre-developed mouse β-actin provided endogenous normalization controls (Applied Biosystems, Foster City, CA). The relative quantification calculation is according to ABI user bulletin #2. Briefly, technical triplicates were performed for the CB1R and β-actin real-time PCR and the Ct values were averaged. The target CB1R gene Ct value was subtracted from the endogenous control β-actin Ct value to obtain delta-Ct value for R7T1 and the isolated mouse islet. R7T1 delta-Ct value was subtracted from delta-Ct of mouse islet as control to obtain delta-delta-Ct values. The relative fold change is calculated using the formula $2^{(-\delta\delta Ct)}$. The efficiency of the CB1R and the β-actin probe amplifications was validated to be proximately equal against different concentration of total RNA.

2.6 Immunofluorescence

Indirect immunofluorescence staining for the CB1R on RT1 cells was performed as described previously [4] using the rabbit anti-CB1R antibody (1:100) from Frontier Science Co. Ltd. (Hokkaido, Japan).

2.7 Statistical Analysis

Unless stated otherwise, means ± sem are given, and Student's *t* test was used to determine statistical significance between two values.

3. Results

3.1 Delayed rectifier currents

Delayed rectifier currents were readily observed in β-cells (Fig. 1A, inset). Direct application of 2-AG to recorded β-cells resulted in a tendency toward a faster decay of these currents (Fig. 1A, inset), therefore the integral of the current, rather than the peak current was used to measure these responses. We found that 2-AG inhibited delayed rectifier currents in β-cells in a concentration-dependent manner (Fig. 1A), and that a 50 % blockade of this current (IC_{50}) by 2-AG was estimated to occur at 20 μM.

To determine if blockade of the delayed rectifier by 2-AG was mediated by cannabinoid receptors, we tested the cannabinoid receptor agonist WIN55,212-2 and its inactive enantiomer WIN55,212-3. We used a concentration (1 μM) which we had previously shown WIN55,212-2 can fully activate CB1Rs in the brain [10]. Both WIN55,212-2 and WIN55,212-3 slightly blocked the delayed rectifier currents in β-cells (to 93.4 ± 1.6 % of control, n=7; 90.5 ± 4.3, % of control, n=6, respectively), but the difference in activity between these two drugs was insignificant(t = 0.68; P =0.51, Fig. 1B). Since WIN55,212-3 is inactive at CB1R [11], we conclude that the effects of these drugs on the delayed rectifier were not mediated by this receptor.

3.2 High voltage activated calcium currents

Initial experiments showed that the L-type calcium channel blocker nifedipine (10 μM) blocked 55.6 ± 2.3% (n=15) of the current activated using this approach, indicating that this L-type calcium channels form the majority of the HVA calcium currents in this β-cell line. In contrast, ω-Conotoxin GVIA (1 μM) produced no effect in 8 of 9 cells tested. Therefore, we conclude that N type channels are largely absent in this β-cell line.

Similar to the delayed rectifier currents, 2-AG reduced HVA currents with an IC_{50} of 20 μM (Fig. 1C). To determine whether this effect was mediated by cannabinoid receptors, WIN55,212-2 and WIN55,212-3 were tested (1 μM). Fig. 1D shows that though the two drugs caused a 16.0 ± 1.5 % (n=13) and 19.1 ± 2.1% (n=13) block, respectively, of the HVA calcium current, the difference was not significant (t = 1.204; P (two-tail) = 0.24). By the same argument applied to the delayed rectifier above, we conclude that the effects of these drugs on HVA currents were not mediated by activation of this receptor.

3.3 2-AG blocked K_{ATP} channels

The inside-out membrane patch configuration was used to examine single ion channel properties in R7T1 β-cells. K_{ATP} channels identity was verified by single channel amplitudes of 3.7 to 4.7 pA (at +60 mV), and by complete inhibition by ATP (1 mM).[12] The EC 2-AG inhibited K_{ATP} channels with an IC_{50} of 1μM (Fig. 2A).

Because recordings under control condition revealed multiple K_{ATP} channels per patch, and rarely a single active channel, our analysis of the blocking mechanism of 2-AG was

confined to within-burst kinetic dwell-time analysis and channel open probability (P_O). The within burst P_O, evaluated from the all-points histogram, ranged from 0.82 to 0.87. As an independent corroboration, the difference between this value and the estimate derived from dwell time analysis ($P_O = tau_{open}/(tau_{open} + tau_{closed})$ was < 3 %. Analysis of within burst channel kinetics, (Fig 2B–2D), showed that within-burst dwell times were unaffected by 10 μM 2-AG (Table 1). The time course of a typical experiment is shown in figure 3(A and E). In this example, the current was completely inhibited by 1 mM ATP and rebounded to 21 pA upon washing. 2-AG (10 μM) inhibited the activity to 7 pA (Fig 3A), accompanied by a decrease in the number of active channels from 7–8 to 2–4 while the open channels probability (P_O) decreased from approximately 0.7 to 0.2 (Fig 3E). The analysis of P_O is exemplified in Fig. 3B–D, which shows the current under control condition (at the dot in panel A), the all points histogram (Fig. 3C), and the comparison of the experimental fractional areas of each component (open bars) to the binomial fit with $P_O = 0.72$ (crosshatched bars) in Fig. 3D. At a few times (triangles in Fig. 3E) two different open probabilities were favored by log likelihood analysis, indicating that in a single patch two different probabilities could appear simultaneously. Data from five patches were analyzed with the same detail as exemplified by Fig. 3, and though initial open probabilities varied from 0.13 to 0.68, 2-AG (10 μM) decreased the open probability to 18.7 ± 0.9% of whatever the initial values was. In addition, the number of open channels decreased to 49 ± 9%. These factors account for reduction of channel activity to 0.19 × 0.49 = 0.09 of the control value, which compares well to the mean activity of 0.06 seen Fig. 3.

Because 2-AG was superfused to the cytosolic side of the membrane in these inside-out patches, its block could be mediated through a receptor-independent action or, transduced by a cannabinoid receptor. To test the latter possibility, the CB1R antagonist AM251 (10 μM) was added to the pipette solution while 2-AG (3 μM) was superfused onto the patch. Given a Ki for AM251 of 7.5 nM[13] and a Ki for 2-AG of 472 nM,[14]when these two drugs are in competition this concentration of AM251 should block 99.5% of the 2-AG response. In 8 cells, 2-AG (3 μM) gave a 79 ± 8% block in the presence of AM251, compared to the 77 ± 2% block given for the same 2-AG concentration alone. This result indicates that the CB1R did not mediate the 2-AG block of the K_{ATP} channel at low concentration of glucose. The concentration-response curve (Fig. 2), fitted to the Hill equation, gave a $IC_{50} = 1.05 \pm 0.19$ μM and a Hill coefficient of 1.17 ± 0.26.

To confirm that the R7T1 cell line does indeed express the CB1R we tested for the presence of both the transcript and protein of this gene. We examined mRNA using qRT-PCR, and compared these measures to those obtained in wildtype mouse islets. Fig. 4A shows qRT-PCR data showing expression of CB1R was 14-fold higher in R7T1 cells than that found in isolated islets from wild-type mice. Furthermore, the cells were found to express the CB1R protein by immunofluorescence (Fig 4B).

4. Discussion

The present study demonstrates that the EC 2-AG could reduce membrane currents mediated by delayed rectifier potassium channels, HVA calcium channels, and K_{ATP} channels. Blockade of these channels was shown to be independent of the cannabinoid receptors by use of synthetic cannabinoid receptor agents. The most significant of these effects was observed on the K_{ATP} channel, which was blocked 50% by 2-AG (1 μM) and was found to be independent of the CB1R by use of the highly specific CB1R antagonist AM251.

2-AG blocked the delayed rectifier in the R7T1 cell line independently of cannabinoid receptors with an IC_{50} of 20 μM. The predominant delayed potassium channel in murine β-cells is the $K_{V2.1}$ type,[15] and we were unable to find any reports of its blockade by ECs

either in the β-cell or any other cell type. In addition to $K_{V2.1}$ there is evidence for six other potassium channels on β-cells[16], including $K_{V1.5}$. Moreno-Galindo and colleagues[17]have shown that the $K_{V1.5}$ channel is blocked by the EC anandamide at an extracellular IC_{50} of 2 μM and conclude that it directly blocks the open channel from the intracellular side. Poling and co-workers[18] have shown that 3 to 10 μM anandamide blocks the $K_{V1.2}$ channel (not found in β-cells) independently of cannabinoid receptors.

In the only functional study, Oz and co-workers [19], using a transverse tubule membrane assay, showed that the loss of $^{45}Ca^{++}$ driven by low potassium-driven depolarization was reduced by one-half when the vesicle preparation was treated with 10 μM 2-AG. Furthermore, binding studies have shown that ECs can bind to L-type calcium channels in the IC_{50} range of 3.2 to 15 μM. [19–21] Both of these reports are consistent with our finding that 2-AG blocks high voltage activated channels of the R7T1 cell line at an IC_{50} of 20 μM.

The K_{ATP} channel, with IC_{50} of 1 μM, was the most sensitive of the currents we examined to blockade by 2-AG. Given the gatekeeper role of this channel in the mechanism of insulin secretion, this high sensitivity was particularly noteworthy. The effect of 2-AG on the K_{ATP} channel was to diminish the channel open probability, P_O. On adding 2-AG, some channels dropped out completely so that a diminished number of open channel currents were active. In addition, the open probability of the remaining active channels was diminished, and the combination of dropped-out channels and reduced open probability was sufficient to account for the block at 10 μM 2-AG. In some instances, the active channels in a single patch had two different open probabilities (e.g. Fig 3E). In no instance, however, were the open and closed dwell times within a burst altered by 2-AG (Table 1; Figure 2C–D), thereby limiting the effects of 2-AG to the ensemble of closed kinetic states.

Of the three currents examined, the block of the K_{ATP} channel was the most significant. The direct blockade of the K_{ATP} channel by 2-AG at low glucose would depolarize the cell and thereby stimulate insulin secretion. Therefore 2-AG could be classified as an initiator of insulin secretion, stimulating insulin secretion in a manner similar to that of the suphonylureas that also directly interact with the K_{ATP} channel. Closure of the K_{ATP} channel, in depolarizing the cell, would precipitate an increase in intracellular calcium (the precursor to insulin secretion). Indeed Li and co-workers recently showed that the endocannabinoid AEA (1μM) when applied to a murine β-cell at low glucose (2mM) increases calcium oscillations.[22] More recently Li and co-workers, using a perifusion system to examine insulin secretion, recently demonstrated that 2-AG (10μM) and the related compound arachidonyl-2′-chloroethylamide (ACEA) could initiate insulin secretion at 2mM glucose.[7] They also show that this could not be reversed by AM251 thus showing that it is CB1R independent. Therefore our result showing a significant blockade of the K_{ATP} channel at low glucose now reveals the underlying foundation for 2-AG-stimulated calcium influx and consequent insulin secretion in the β-cell.

Acknowledgments

M.E.D. was the recipient of the Sanford Career Award granted by the Juvenile Diabetes Research Foundation (JDRF) in collaboration with the Sanford Project for Type 1 Diabetes, Sioux Falls SD. M.E.D. was also funded by JDRF innovative award # 26-2008-864 and by a special grant from Autoimmunity Fund at Johns Hopkins, Division of Endocrinology. This work was supported in part by the Intramural Research Program of the National Institute of Drug Abuse (NIDA)/NIH and Intramural Research Program of the National Institute on Aging (NIA)/NIH.

References

1. Piomelli D. The molecular logic of endocannabinoid signalling. Nat Rev Neurosci. 2003; 4:873–884. [PubMed: 14595399]

2. Howlett AC, Barth F, Bonner TI, Cabral G, Casellas P, Devane WA, Felder CC, Herkenham M, Mackie K, Martin BR, Mechoulam R, Pertwee RG. International Union of Pharmacology. XXVII. Classification of cannabinoid receptors. Pharmacol Rev. 2002; 54:161–202. [PubMed: 12037135]
3. Di Marzo V, Bifulco M, De Petrocellis L. The endocannabinoid system and its therapeutic exploitation. Nat Rev Drug Discov. 2004; 3:771–84. [PubMed: 15340387]
4. Kim W, Doyle ME, Liu Z, Lao Q, Shin YK, Carlson OD, Kim HS, Thomas S, Napora JK, Lee EK, Moaddel R, Wang Y, Maudsley S, Martin B, Kulkarni RN, Egan JM. Cannabinoids Inhibit Insulin Receptor Signaling in Pancreatic {beta}-Cells. Diabetes. 2011; 60:1198–11209. [PubMed: 21346174]
5. Bermudez-Silva FJ, Suarez Perez J, Nadal A, Rodriguez de Fonseca F. The role of the pancreatic endocannabinoid system in glucose metabolism. Best Pract Res Clin Endocrinol Metab. 2009; 23:87–102. [PubMed: 19285263]
6. Oz M. Receptor-independent actions of cannabinoids on cell membranes: focus on endocannabinoids. Pharmacol Ther. 2006; 111:114–144. [PubMed: 16584786]
7. Li C, Bowe JE, Huang GC, Amiel SA, Jones PM, Persaud SJ. Cannabinoid receptor agonists and antagonists stimulate insulin secretion from isolated human islets of Langerhans. Diabetes Obes Metab. 2011; 13:903–910. [PubMed: 21564460]
8. Li C, Bowe JE, Jones PM, Persaud SJ. Expression and function of cannabinoid receptors in mouse islets. Islets. 2010; 2:293–302. [PubMed: 21099327]
9. Glasbey CA, Martin RJ. The distribution of numbers of open channels in multi-channel patches. J Neurosci Methods. 1988; 24:283–287. [PubMed: 2458512]
10. Laaris N, Good CH, Lupica CR. Delta9-tetrahydrocannabinol is a full agonist at CB1 receptors on GABA neuron axon terminals in the hippocampus. Neuropharmacology. 2010; 59:121–127. [PubMed: 20417220]
11. D'Ambra TE, Estep KG, Bell MR, Eissenstat MA, Josef KA, Ward SJ, Haycock DA, Baizman ER, Casiano FM, Beglin NC. Conformationally restrained analogues of pravadoline: nanomolar potent, enantioselective, (aminoalkyl)indole agonists of the cannabinoid receptor. J Med Chem. 1992; 35:124–135. [PubMed: 1732519]
12. Ashcroft FM. Adenosine 5′-triphosphate-sensitive potassium channels. Annu Rev Neurosci. 1988; 11:97–118. [PubMed: 2452599]
13. Lan R, Liu Q, Fan P, Lin S, Fernando SR, McCallion D, Pertwee R, Makriyannis A. Structure-activity relationships of pyrazole derivatives as cannabinoid receptor antagonists. J Med Chem. 1999; 42:769–776. [PubMed: 10052983]
14. Mechoulam R, Ben-Shabat S, Hanus L, Ligumsky M, Kaminski NE, Schatz AR, Gopher A, Almog S, Martin BR, Compton DR. Identification of an endogenous 2-monoglyceride, present in canine gut, that binds to cannabinoid receptors. Biochem Pharmacol. 1995; 50:83–90. [PubMed: 7605349]
15. MacDonald PE, Wheeler MB. Voltage-dependent K(+) channels in pancreatic beta cells: role, regulation and potential as therapeutic targets. Diabetologia. 2003; 46:1046–1062. [PubMed: 12830383]
16. Jacobson DA, Weber CR, Bao S, Turk J, Philipson LH. Modulation of the pancreatic islet beta-cell-delayed rectifier potassium channel Kv2.1 by the polyunsaturated fatty acid arachidonate. J Biol Chem. 2007; 282:7442–7449. [PubMed: 17197450]
17. Moreno-Galindo EG, Barrio-Echavarria GF, Vasquez JC, Decher N, Sachse FB, Tristani-Firouzi M, Sanchez-Chapula JA, Navarro-Polanco RA. Molecular basis for a high-potency open-channel block of Kv1.5 channel by the endocannabinoid anandamide. Mol Pharmacol. 2010; 77:751–758. [PubMed: 20133392]
18. Poling JS, Rogawski MA, Salem N Jr, Vicini S. Anandamide, an endogenous cannabinoid inhibits Shaker-related voltage-gated K+ channels. Neuropharmacology. 1996; 35:983–991. [PubMed: 8938728]
19. Oz M, Tchugunova Y, Dinc M. Differential effects of endogenous and synthetic cannabinoids on voltage-dependent calcium fluxes in rabbit T-tubule membranes: comparison with fatty acids. Eur J Pharmacol. 2004; 502:47–58. [PubMed: 15464089]

20. Johnson DE, Heald SL, Dally RD, Janis RA. Isolation, identification and synthesis of an endogenous arachidonic amide that inhibits calcium channel antagonist 1,4-dihydropyridine binding. Prostaglandins Leukot Essent Fatty Acids. 1993; 48:429–437. [PubMed: 8341720]

21. Shimasue K, Urushidani T, Hagiwara M, Nagao T. Effects of anandamide and arachidonic acid on specific binding of (+) -PN200-110, diltiazem and (−) -desmethoxyverapamil to L-type Ca2+ channel. Eur J Pharmacol. 1996; 296:347–350. [PubMed: 8904088]

22. Li C, Jones PM, Persaud SJ. Cannabinoid receptors are coupled to stimulation of insulin secretion from mouse MIN6 beta-cells. Cell Physiol Biochem. 2010; 26:187–196. [PubMed: 20798502]

- We examined how the endocannabinoid 2-AG influences β-cell ion channels at 2mM glucose.
- 2-AG inhibited the HVA calcium (the majority of which are L-type channels), K_V, and K_{ATP} channels.
- Blockade of all these channels was independent of cannabinoid receptors.
- The K_{ATP} channel was the most sensitive to 2-AG blockade; the IC_{50} is 1μM.
- This provides a mechanism for how ECs can increase insulin secretion at 2mM glucose.

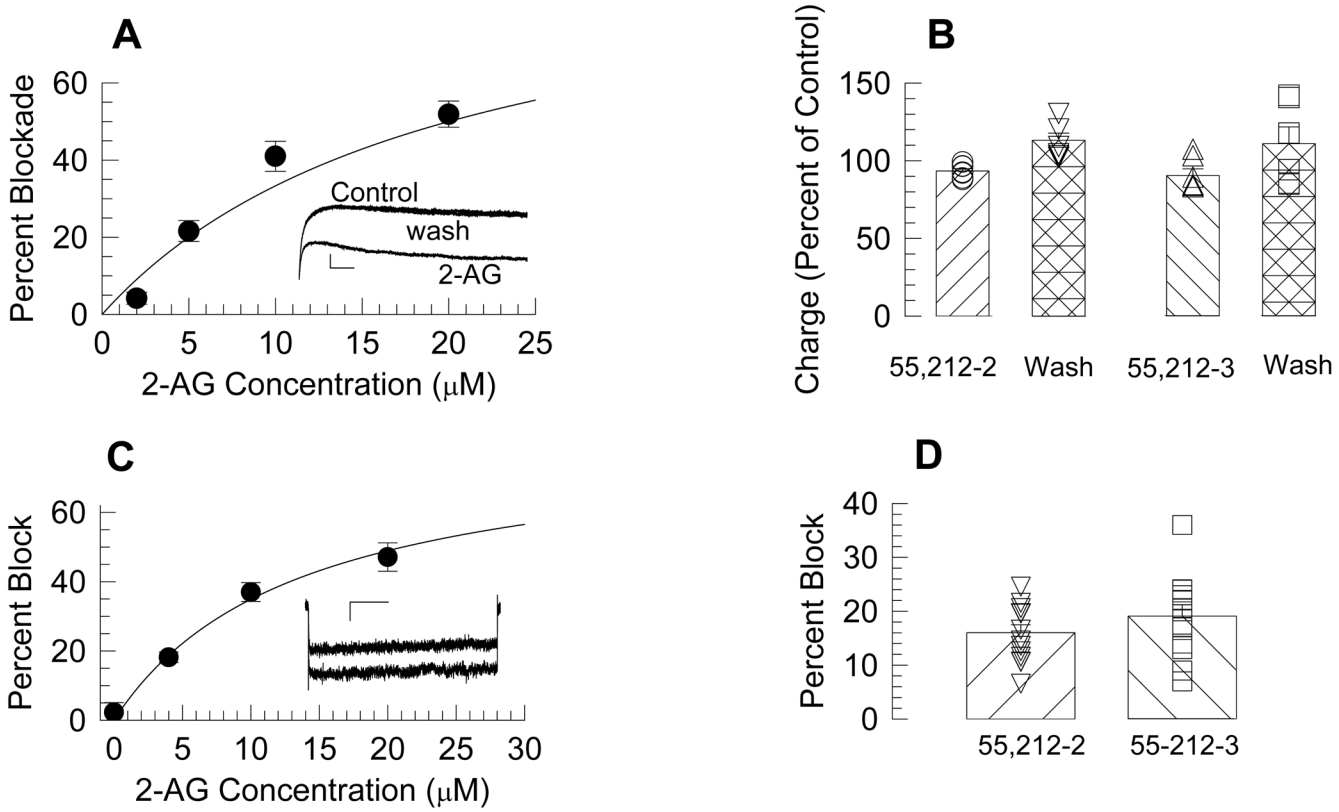

Figure 1. 2-AG blocked delayed rectifier and high voltage activated calcium currents

A: Concentration response curve for 2-AG blockade of the delayed rectifier. Each point represents the mean ± sem of 11 to 14 cells. The inset shows current traces under control, 2-AG (10 μM), and wash conditions. Calibration bars represent 500 pA and 20 ms. B: The CB agonist WIN55,212-2 and its inactive inantiomer produced small and equal decrements.. C: Concentration response curve for 2-AG blockade of high voltage activated calcium currents. Each point represents the mean ± sem of 8–13 cells. The inset shows representative currents under control condition (lower) and in the presence of 10 μM 2-AG. The calibration bars represent 30 pA and 200 ms. D: Both WIN55,212-2 and WIN55,212-3 (1 μM) blocked the HVA calcium currents by equal amounts. Bars represent the mean and the error bars sem, and symbols values from separate cells.

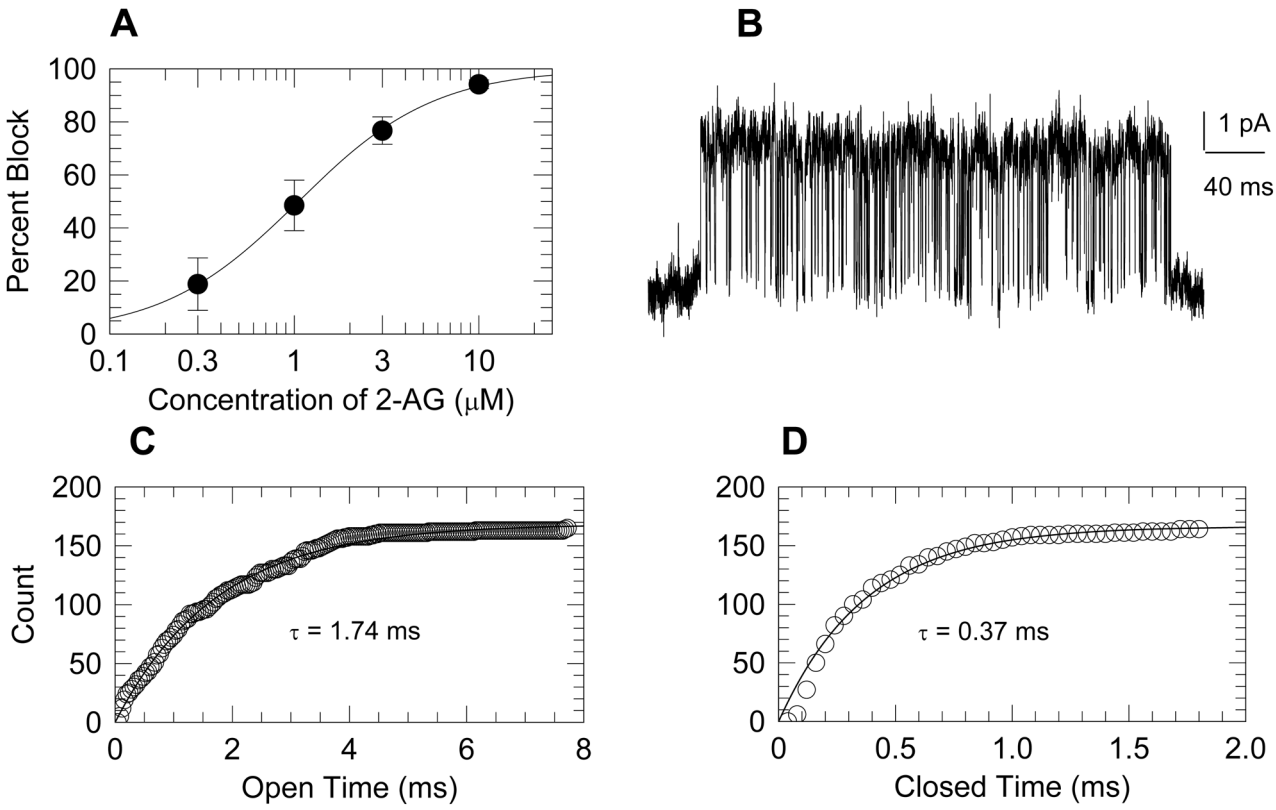

Figure 2. 2-AG blocked K_{ATP} channels

A: Concentration response curve for the blockade of K_{ATP} channels by 2-AG. Symbols represent the mean ± sem of 7 to 11 patches. B: An example of a KATP channel burst under control conditions. C and D: Open and closed dwell times for the single burst, shown in panel B, are plotted as cumulative histograms. The experimental points are shown as symbols, and fitted exponential curves are shown as smooth curves.

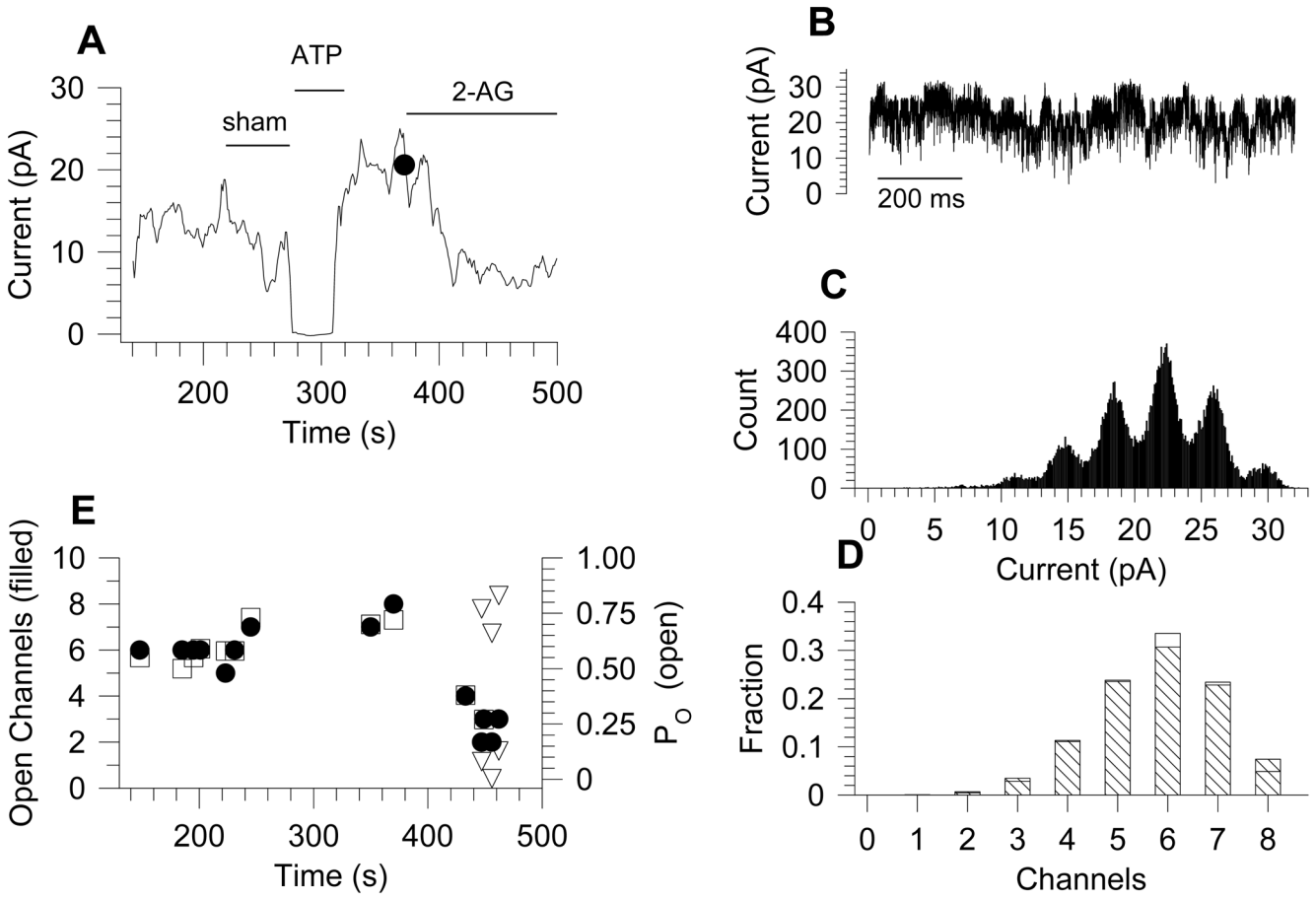

Figure 3. Binomial analysis of K_{ATP} channel currents

A: averaged currents as a function of time. A sham solution change produced no change in current, whereas 1 mM ATP inhibited it completely. Upon washing, the current rebounded to a higher level. 2-AG (10 μM) reduced activity. An example of the binomial analysis sampled at the dot is shown in panels B – D. B: The 1s current sample taken for analysis. C: The all points amplitude histogram shows 8 active channels of 3.70 pA. D: The fraction areas found in C are shown as open bars compared to values predicted from binomial analysis with 8 active channels and open probability of 0.72. Log likelihood analysis using 9 channels gave a poorer fit. E: Plot of the time course of the number of active channels and their open probabilities for the same experiment shown in panel A. During treatment with 2-AG, some binomial analyses using a single open probability were better fitted by using the generalized binomial distribution, which yielded two different P_O values, indicated by the triangles.

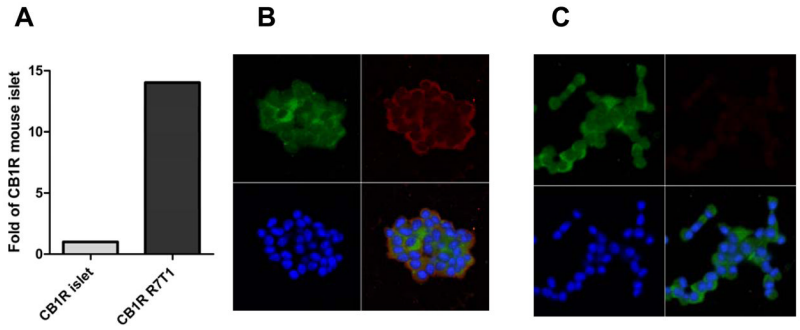

Figure 4. Presence of CB1 receptors on R7T1 cells

A: RT-qPCR shows that the level of CB1R mRNA present in R7T1 is 14-fold higher in R7T1 cells that in mRNA from intact mouse islets. Levels are normalized to β-actin. B: Representative immunostaining for CB1R and insulin as indicated in the R7T1 cells shows that staining in confined to the membrane. Green (FITC) insulin, Red (Red-X) CB1R, blue, TO-PRO-3 C: Specificity of the staining for the CB1R assessed by using the secondary antibody alone. Scale bar = 50 μm. Lower right quadrants are superpositions of the other three channels.

Table 1

Analysis of within-burst single channel kinetics under control condition and in the presence of 10 μM 2-AG.

	Open Time (ms)	Closed Time (ms)	Total Events	Patches
Control	1.73±0.02	0.35±0.01	5,681	3
2-AG	1.78±0.02	0.34±0.01	8,395	4